JOINT INSTITUTE FOR NUCLEAR RESEARCH
Frank Laboratory of Neutron Physics

FINAL REPORT ON THE INTEREST PROGRAM

Coexistence of superconductivity and ferromagnetism at low-dimensional heterostructures

Supervisor
Dr. Vladimir Zhaketov

Student
Amna Salah Mahmoud

Participation period
February 10 – March 26, 2023
Wave 8

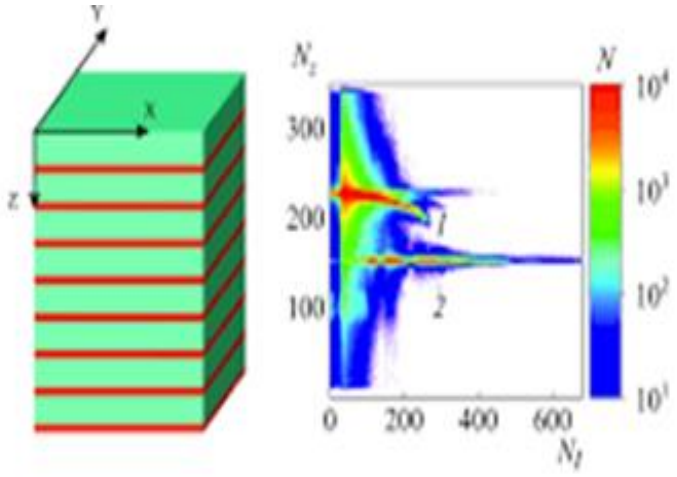

Contents

Abstract

Using the experimental method of polarized neutron reflectometry through the REMUR spectrometer at JINR, and combined with simulations of different nominal structures using MATLAB we studied the Coexistence of Superconductivity and Ferromagnetism at Low Dimensional Heterostructure In addition, we researched changing of neutron and X-ray scattering properties from thickness, magnetization, and several layers using numerical methods. Due to the interaction of neutrons with nuclei and magnetic moments we discussed the influence of the grazing angle of the neutron beam, colinear and non-collinear magnetization, the thickness of the ferromagnetic layer, different ferromagnetic materials, size of the superlattice, and roughness of the structure on the reflectivity spectra. By comparing the different values of mentioned properties and different ferromagnetic materials, we conclude that there is a mutual influence of the ferromagnetic and superconducting layers in the analysed heterostructures.

1. Introduction

1.1 Proximity effects in superconductor-ferromagnet structures

Dutch physicist Heike Kamerlingh Onnes discovered the superconductivity phenomenon in 1911, It is the sudden disappearance of electrical resistance by cooling the material below a characteristic temperature called critical temperature Tc[1]. In 1986, several cuprate-oxide superconductors were discovered, including YBCO, $Bi_2Sr_2CaCu_2O_{8+\delta}$ (BSCCO), and HgTiBaCaCuO, with critical temperatures beyond 77 K.

In 1933, W. Meissner and R. Ochsenfeld found that the superconducting materials expelled the magnetic field from its volume at or below Tc. In contrast, due to the magnetic induction effect, the realizable ferromagnet materials concentrate the field's force lines inside its volume. As competing phenomena, superconducting and ferromagnetic coexist in uniform materials is complex. It requires unique and rugged conditions. Ginzburg[2] proposed the first explanation of the superconductivity suppression via ferromagnetic ordering in the transition metals. He indicated that in these metals, magnetic induction exceeds the critical field.

The proximity effect was defined by P. F. Dahl [3] in 1984, as the partial transfer of superconducting properties to a typical metal as they are connected electrically because of the large spatial extension of the wave function of the Cooper pairs at distances comparable with the coherence length. In contrast, the reverse proximity effect may occur in a ferromagnet (FM)/superconductor (S) heterostructures, which implies magnetization of the superconducting layer. [4] Studies of heterogeneous systems involving ferromagnetic and superconducting materials have been conducted extensively since the publication of the pioneering papers by Z.Radovic et al.[6] and Y.N.Proshin et al.[7], developing the fundamentals of the theory of FM/S junctions. The temperature dependence of the magnetic proximity effect is investigated in [8]. In [5], Nb(25 nm)/Gd/ Nb(25 nm) Tri layers has been studied showing that the structures with highly transparent S/F interfaces and rather high correlation length can be grown. Theoretical results with is used for calculation is represented in[9] .

1.2 Polarized neutron reflectometry

Historically, polarized neutrons were used in the study of the magnetic properties of ferromagnets by neutron depolarization method where the polarization of the transmitted neutron beam through the sample was measured. Currently neutron reflectometry is used on a larger scale for different investigations as magnetic excitations in ferromagnets, structures of magnetic materials, and investigation of solid body surfaces . [10] Fundamentally, the theory behind neutron reflectometry is the scattering of scalar quantum particle with the potential function as the interaction potential between neutrons in the neutron beam and the materials constituting the sample[11].

The apparatus structure Figure 1 is essentially a reactor (source of neutrons), a polarizer(magnetic supermirrors, transmission through polarized gas as He, or transmission through magnetized films), a spin flipper (space varying magnetic field that is constant in time, a combination of radio frequency and constant fields), the sample, another spin flipper followed by a polarization analyser, and finally a detector.

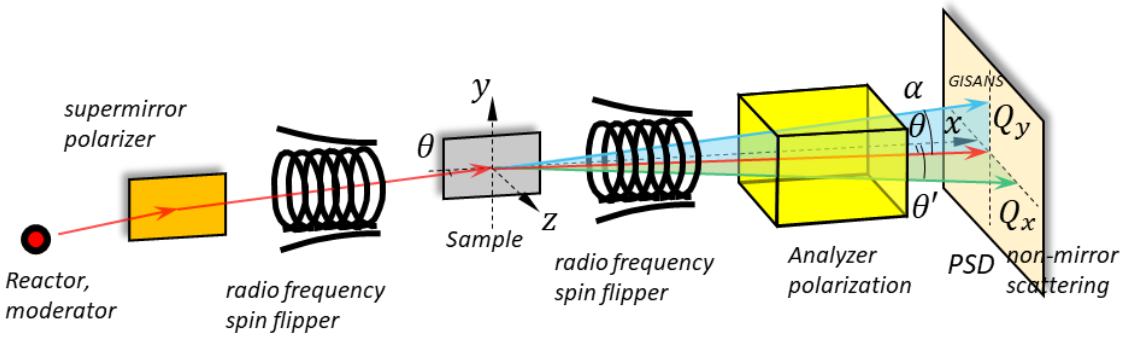

Figure 1 Scheme of reflectometric experiment with full polarization analysis

In this experiment, polarized neutron spectrometer REMUR in Dubna is being used to characterize heterostructures samples [12]. One feature of reflectometry mode in REMUR reactor is that it has spin-flippers tool which allowed observation of spin asymmetry (SA) that might arise such as in proximity effect of superconductivity. Suppression of ferromagnetism due to spilling of cooper pair inside ferromagnet could be deduced by comparing spin asymmetry of S/F heterostructures above and below superconducting transition temperatures . The difference in asymmetry could be attributed to

electromagnetic origin. The setup has been used to setup experiments in proximity effects in SF heterostructures composed of Gd/Nb layers, $V/Fe_{0.7}V_{0.3}/V/Fe_{0.7}V_{0.3}/Nb$ and $Nb/Ni_{0.65}(0.81)\ Cu_{0.35}(0.19)$, Dy/Ho thin films, and V (40 nm) /Fe (1 nm) layers[11–20] .

1.3 Aim and methodology

Understanding the problems of coexistence superconductivity/ ferromagnetism by studying low-dimensional heterostructures composed of Niobium (Nb), Gadolinium (Gd), Vanadium (V), Sapphire substrate (AL_2O_3), and other elements Figure **2**, using the numerical simulations of polarized neutron reflectometry method and X-ray method. Main tasks are Processing of the experimental data spectra using Spectra Viewer software, Data fitting with the physical model using MATLAB software, and modelling of reflectivity curve depending on different parameters. In this project, there were several software which was utilized to simulate and calculate numerical value. For instance, To open and extract numerical data of the neutron reflectometry experiment, Spectra Software was used. X'Pert Reflectivity software was used to simulate X-Ray reflectivity from heterostructures layers. In addition, numerical calculation and simulation of neutron reflectivity were performed by MATLAB using Lemur.m file provided by Dr. Zhaketov. Finally. plotting and several calculations were carried out using OriginLab.

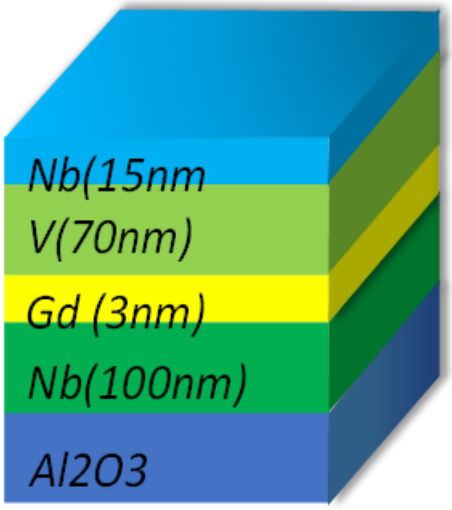

Figure 2 Low dimensional hetero-structure

2. Tasks

2.1 Task 1 : fitting experimental data

Using the experimental data of the reflectivity of plus (spin flipper on) and minus (spin flipper off) polarized neutrons, collected by the REMUR spectrometer at two different temepratures (1.5K below Tc, 12K above Tc) for the nominal structure Al2O3 / Nb(100nm) / Gd(3nm) / V(70nm) / Nb(15nm). The numerical values of these data was extracted using Spectra Viewer software and exported to OriginLab. The spin asymmetry was calculated from the experimental data using the following equation:

$$SA = \frac{R_+ - R_-}{R_+ + R_-} \qquad 1$$

The wavelength of the experimental data was measured by using the following formula:

$$\lambda[\text{Å}] = \frac{(N+35-12)\cdot 3.956\cdot 256}{34030} \qquad 2$$

After performing calculation and plotting of experimental data, neutron reflectivity data were compared with the theoretical data resulting from simulation of the same nominal structure by the lemur program in MATLAB, using 6 mrad grazing angle of neutron, the results are shown in **Figure 3**.

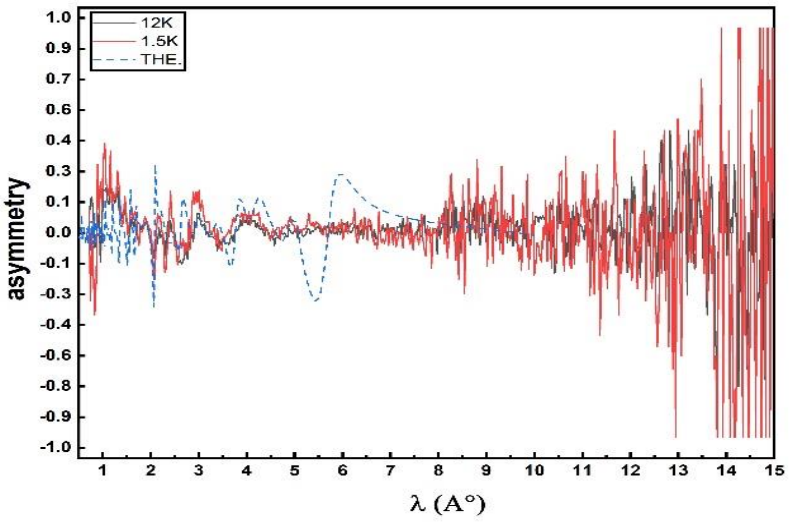

Figure 3 Experimental and Theoretical spin asymmetry at 1.5K and 12K

From **Figure 3** it can be concluded that spin asymmetry of experimental result and simulation are closely matched and due to differing asymmetry values, in either case, it was assumed that spin asymmetry value arises in superconductivity layers due to ferromagnetic suppression of Gd layers (inverse proximity effect), and we also notice large variation in the spin asymmetry at the end part of the experimental plot which is due to the small numbers of the neutrons at this range of wavelength (above 10 angstrom) .

2.2 Task 2 : Comparing reflectivity at different grazing angles

Based on the following formula, the reflectivity of neutrons is related to the radiation angle,

$$Q = \frac{4\pi}{\lambda}\sin(\theta) \qquad 3$$

In this part we examined through simulation how different grazing angles for the beam affects the reflectivity of the neutrons, for Al_2O_3 / Nb(100nm) / Gd(3nm) / V(70nm) / Nb(15nm) heterostructure with 0 magnetization for all layers (so we expect the graph of plus and minus neutrons to be almost identical due to the absence of magnetization), and we compare reflectivity at grazing angles $\theta = 3,\ 6,\ 12$ mrad for that as shown in **Figure 4**.

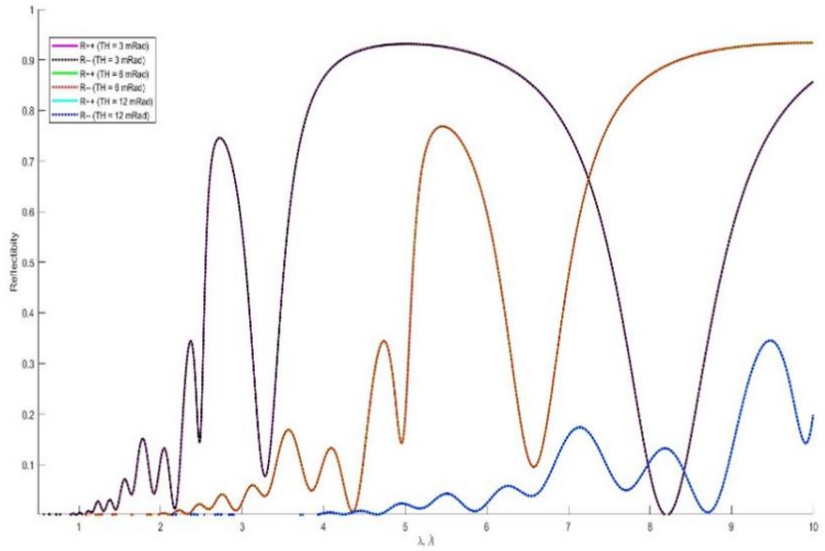

Figure 4 Neutron reflectivity at grazing angles θ = 3, 6, 12 mrad

From **Figure 4** we can observe that The neutrons' momentum is inversely proportional to the incident angle of the neutron beam, Eq.3. So The peaks of the graph shift towards larger wavelengths as we increase the grazing angle. In addition, The amplitude of reflectivity tends to decrease as we increase the angle which is attributed to the decreasing of the intensity of the reflected beam by increasing the grazing angle. Finally , we can notice that the the curves corresponding to the "plus" and "minus" reflectivity of neutrons overlap almost exactly for all angles due to the absence of the magnetization.

2.3Task 3: Comparing reflectivity at different magnetization

In this task we analysed the dependence of the neutron reflectivity on the strength of magnetization and its direction in the of Gadolinium layer (ferromagnetic layer) for :

:

- Collinear case (magnetization parallel to the sample surface only z direction): Mz(Gd) = 100, 1000, 10000 Oe; Mx(Gd)=0, My(Gd)=0

- Non-collinear case: Mx(Gd) = 100, 500, 1000 Oe; Mz(Gd)=1000 Oe , My(Gd)=0, the results related to this problem are presented as follows in Figure 5 and Figure **6**:

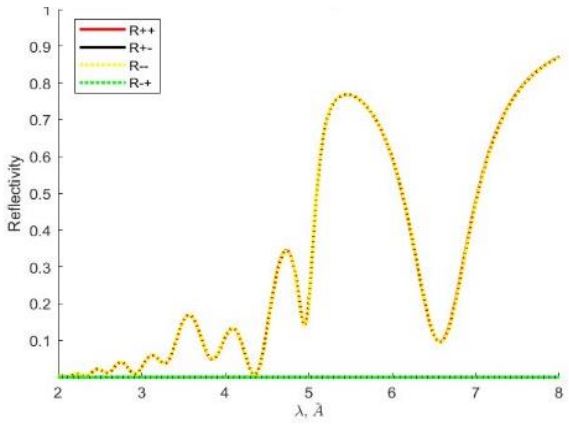

(a) (Mx, My, Mz) = (0, 0, 100)

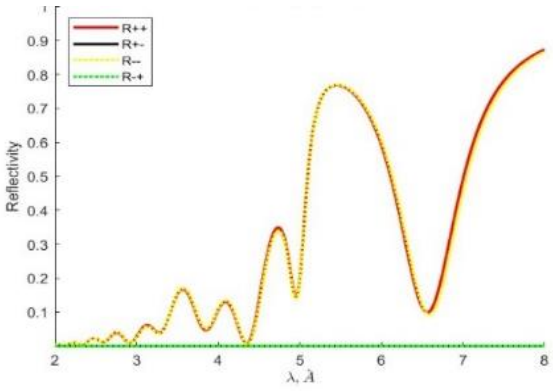

(b) (Mx,My, Mz) = (0, 0, 1000)

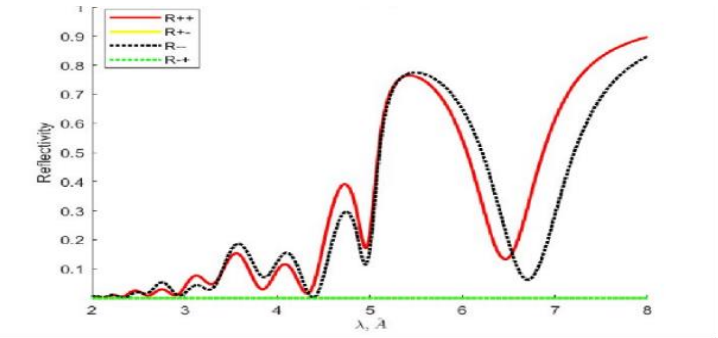

(c) (Mx, My, Mz) = (0, 0, 10000)

Figure 5 (a, b, c)Collinear magnetization

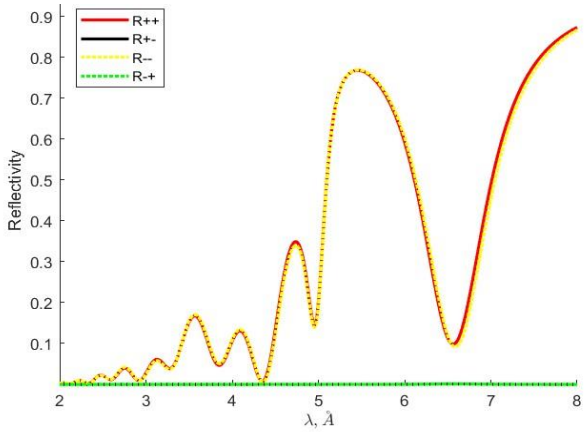

(d) (Mx, My, Mz) = (100, 0, 1000)

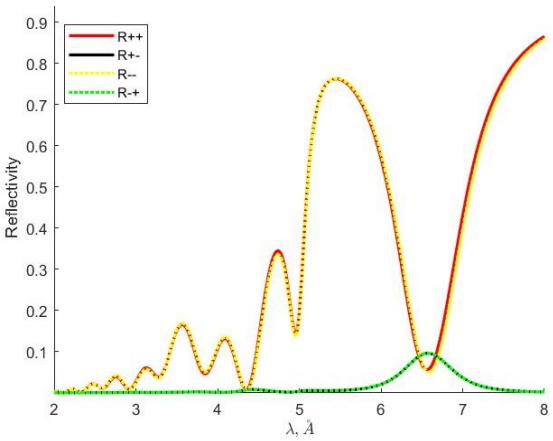

(e) (Mx, My, Mz) = (1000, 0, 1000)

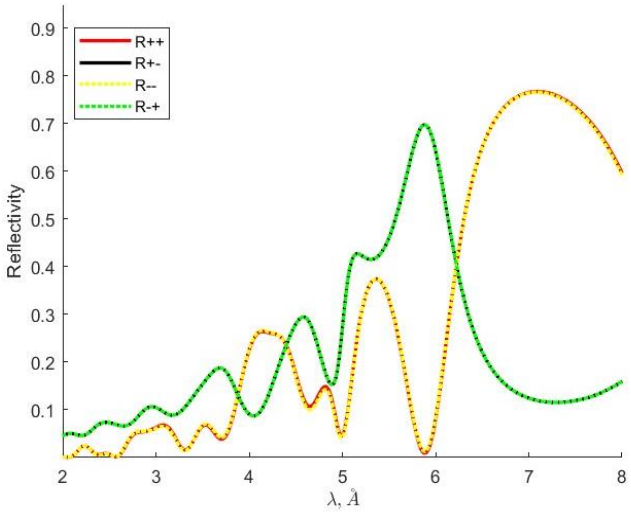

(f) (Mx, My, Mz) = (10000, 0, 1000)

Figure 6 (d, e, f) Non-collinear magnetization

Figure 5 for the collinear case shows that The difference between (plus and minus neutrons) becomes more prominent and apparent as the strength of magnetization increases M_z only (M_X =0 and M_y = 0) which is justifiable as the two neutron kinds differ by a magnetic property. Whereas Figure **6** represents the non-collinear case for Mz=1000 Oe and Mx changes from 100 to 10000 Oe where there no change in the reflectivity graphs, it can be concluded that the polarized neutrons that have occurred remain constant. In addition, by increasing Mx the neutron spin flip will increase and peaks appear. It is worth mentioning, that until Mx=1000, Spin Flips were zero.

2.4 Task 4 : Comparing structures with different thickness (calculation of neutron and X-ray reflectivity)

The third parameter which we analysed is the thickness of the ferromagnetic layer of Gd. The calculation is performed for 12, 30 ,and 60 nm thick at the same grazing angle in the absence of any form of magnetization. Due to the coherence, length of superconductivity, this layer mustn't be too thick. The depth of the penetration of the superconductivity can be a few nanometres in the ferromagnetic layer, we observed how reflectivity is influenced. However we measure the reflectivity for both the neutrons (plus and minus) and a simulated X-ray spectrometer for the same sample as shown in ***Figure 7*** and ***Figure 8***.

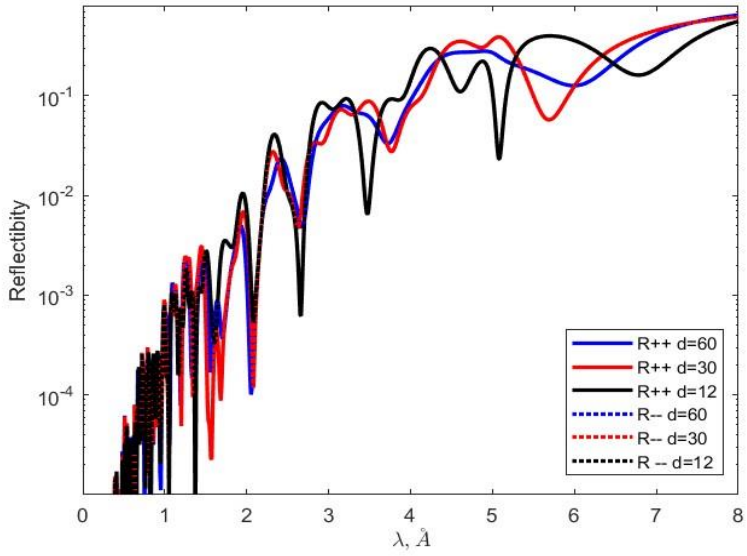

Figure 7 neutron reflectivity of Gd(12, 30, and 60 nm)

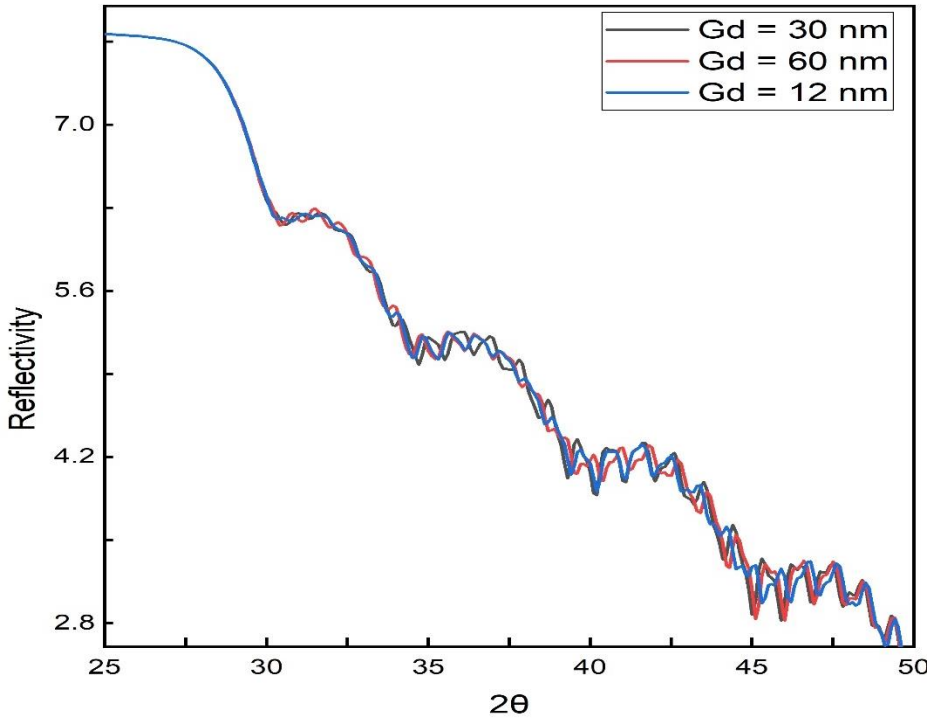

Figure 8 X-ray reflectivity of Gd(12, 30, and 60 nm)

First of all, It can be concluded from *Figure 7* that with the increase in the thickness of the Gd layer, the reflectivity also decreases, so that the maximum peak with a thickness of 3 nm is almost 2 times the maximum peak reflectivity with a thickness of 12 nm, This suppression in the neutron reflectivity for a larger value of thickness could be explained by knowing that for a larger value of thickness, superconducting order parameter inside Gd reached a deeper part of Gd and as such Cooper pair coherence caused more electron to be correlated to cooper pair in superconductors. As such, superconducting layer become thicker which screens ferromagnetic response of Gd layer. In addition, there was no + state and - variations observed in neutron beam simulation since we know that adding more thickness did not change beam interaction with the heterostructures.

On the other hand, X-ray reflectivity does not change much by increasing the thickness of Gd layer Figure 8. Which is acceptable as the Gd layer in the middle of heterostructures does not contribute much to X-ray scattering, as it mainly occurred at the surface. Since we know that X-Ray does not penetrate deeply inside metal then we could safely if addition of thickness of Gd layer does not contribute much to scattering. However, the intensity of X-ray reflectivity tends to decrease by increasing the incident angle.

2.5 Task 5 : Comparing structures with different ferromagnets (calculation of neutron and X-ray reflectivity)

As to this task, the reflectivity of the neutron, as well as X-Ray, were simulated with variations of ferromagnetic layers for following structures:

Al2O3 / Nb(100nm) / Gd(3nm) / V(70nm) / Nb(15nm)

Al2O3 / Nb(100nm) / Fe(3nm) / V(70nm) / Nb(15nm)

Al2O3 / Nb(100nm) / Co(3nm) / V(70nm) / Nb(15nm)

Where there was no magnetizations and the grazing angle was constant = 6 mrad, the results are shown in Figure **9** and Figure 10.

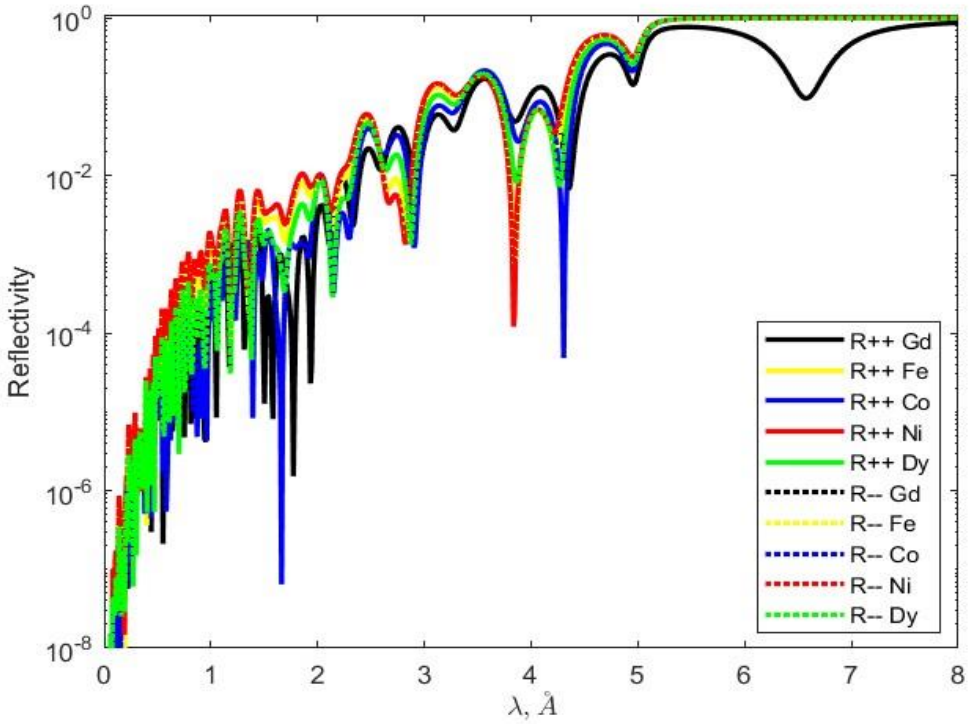

Figure 9 Neutron reflectivity for GD, Fe, Ni, Co, Dy(3nm)

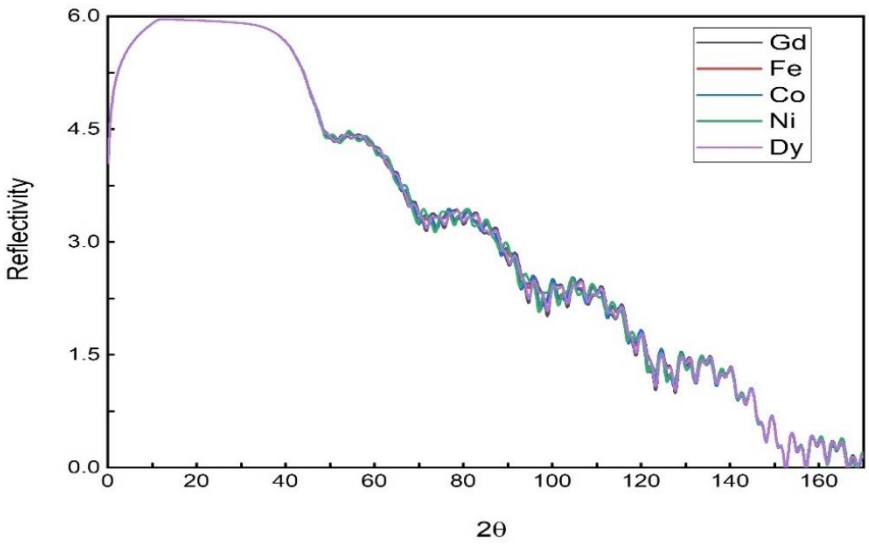

Figure 10 X-ray reflectivity for GD, Fe, Ni, Co, Dy(3nm)

The simulations show that neutron reflectivity has variational reflectivity in each peak of the upper left **Figure 9**. Variational reflectivity below 5 Angstrom happened because ferromagnetism in the layer had various magnetic moment values. As such it has a differing effect on the proximity effect in the superconductivity. Gadolinium has a different neutron reflectivity value because in Gd/Nb layer, Er ~ Es and as such allow rather a large proximity effect where Gd has superconductivity inside it. As a result, it screened out incoming neutron and has lower reflectivity. On the other hand, there is no change in the x-ray reflectivity due to elemental variations. As explained previously, this can be attributed to the location of the elements which were in the middle of heterostructures, and because of that, it did not contribute significantly to x-ray scattering.

2.6 Task : Superlattice (calculation of neutron and X-ray reflectivity)

In this task we evaluated the reflectivity changing for the determined super lattices of this specific layer coupling by coupling Gd (ferromagnetic) and Nb (superconductor) elements as a specific layer and repeating them several times. we have drawn the graph of the changes X-Ray and Neutron reflectivity for the following structures:

Al2O3 / [Nb(25nm) / Gd(3nm)] x10 / Nb(15nm)
Al2O3 / [Nb(25nm) / Gd(3nm)] x20 / Nb(15nm)
Al2O3 / [Nb(25nm) / Gd(3nm)] x30 / Nb(15nm)

Where the was No Magnetization and θ = 6 mrad, the results related to this problem are presented in Figure 11 and Figure 12.

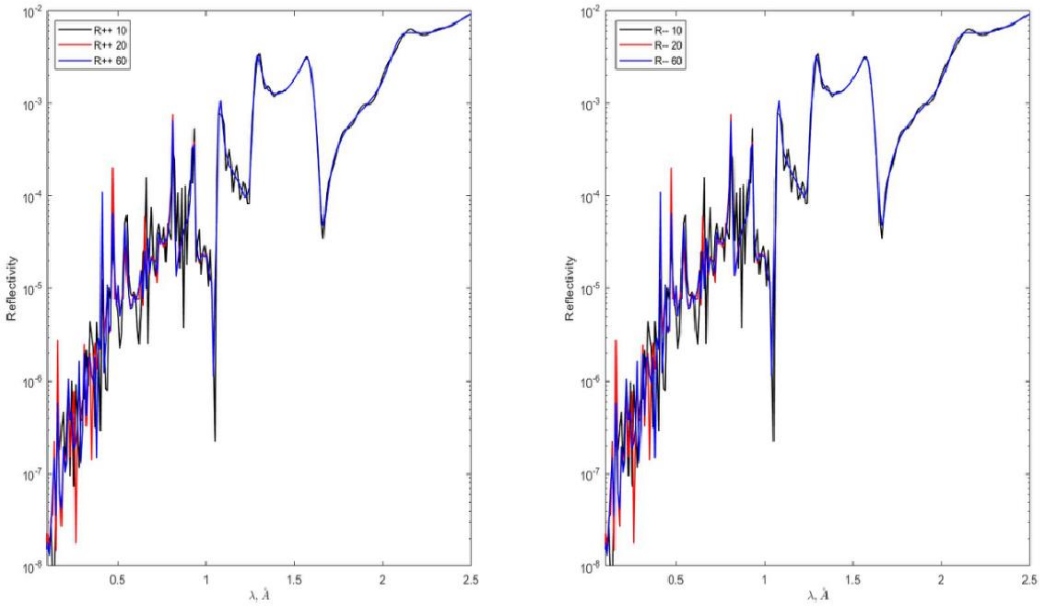

Figure 11 Calculation of neutron for [Nb(25nm) / Gd(3nm)] x10, 20, 30

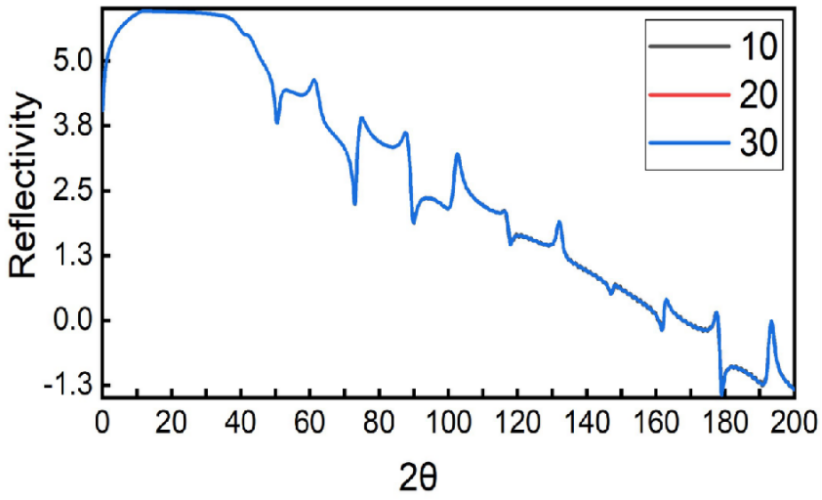

Figure 12 Calculation of X-Ray for [Nb(25nm) / Gd(3nm)] x10, 20, 30

According to Figure 11, it can be concluded that the more the number of pairs of layers increases, the intensity of the neutron reflectivity also increases. This can be explained as more pairs of these layers exist in the structure, the more intense the reflection maxim due to the stronger coupling of ferromagnetism and superconductivity which is happening due to the pairing of electrons from these layers into pairs. One of the electrons is in

the F layer and the second one is in the S layer but with opposite oriented spin.

It is shown from Figure 12 that the intensity of X-rays has not changed with increasing the repetition of the layers this is can be attributed to the X-Ray penetration depth which was quite low for a sample that has a large surface electronic density of states such as transition metal. In contrast with X-Ray, the addition of more heterostructures layers gave rise to a larger value of neutron reflectivity because neutron has a larger penetration depth than X-Ray. so that, when we add more layers to the samples, then we would expect to have a more nuclear magnetic moment which could scatter neutron.

2.7 Task 7: Influence of roughness (calculation only X-ray reflectivity)

Like it is mentioned above, the penetration of X-ray beams in metallic material is small so it interacts on the surface and we can discuss the roughness of the layers. The X-ray spectra for different roughness of 0, 1, 2, and 3 nm for the Al2O3/[Nb(25nm)/Gd(3nm)]$_{20}$/Nb(15nm) heterostructure are shown in Figure 13.

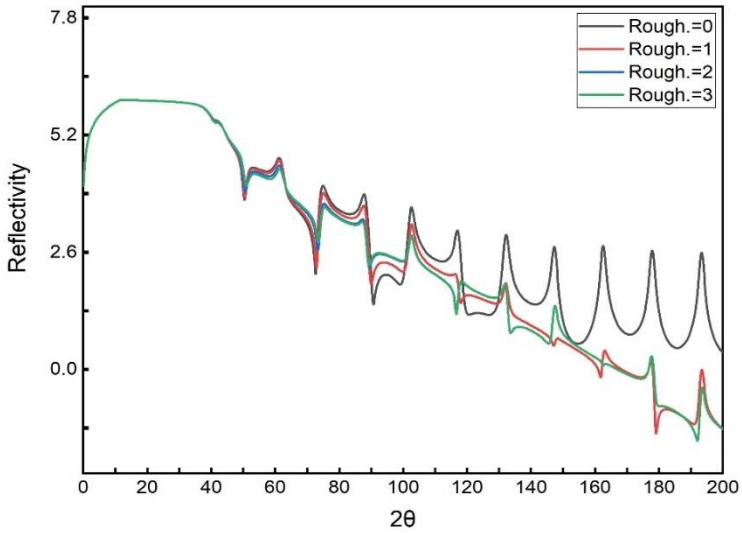

Figure 13. X-ray reflectivity for investigated heterostructures with the roughness of Gd layer of 0, 1, 2, and 3 nm.

From Figure 13, we can observe that with the increase in roughness, the peaks and fluctuations of the graph related to the X-ray intensity for different incident angels decrease and the graph looks smoother, this can be explained by X-ray scattering experiments which often relied on the fact that detectors could only detect scattered beams that arrived at it, including superposition of beam due to lattice scattering of multilayers samples. If samples have

some defects or inhomogeneity, then scattered beams would display reduced intensity because of destructive interference of reflected beams. So that, for a larger value of roughness more beams were getting destructive interference and at the same time scattered to different directions, thus reducing the intensity of beams that arrived at the sample.

2.8 Task 8: Structure with helicoidal magnetic (calculation only of neutron reflectivity)

In this task, studied the variation of the reflectivity for the Dy element with helicoidally magnetic properties (ie element Dy), we have drawn the diagram of neutron reflectivity changes for Mz=Mx=100, Structure with helicoidally magnetic by calculation only of neutron reflectivity for following structure:

Al2O3 / Nb(100nm) / Dy(3nm) / V(70nm) / Nb(15nm)

And Separate Dy-layer to 20 sublayers, with Mz and Mx modulate helicoid The figure of the results related to this problem are presented in Figure 14 :

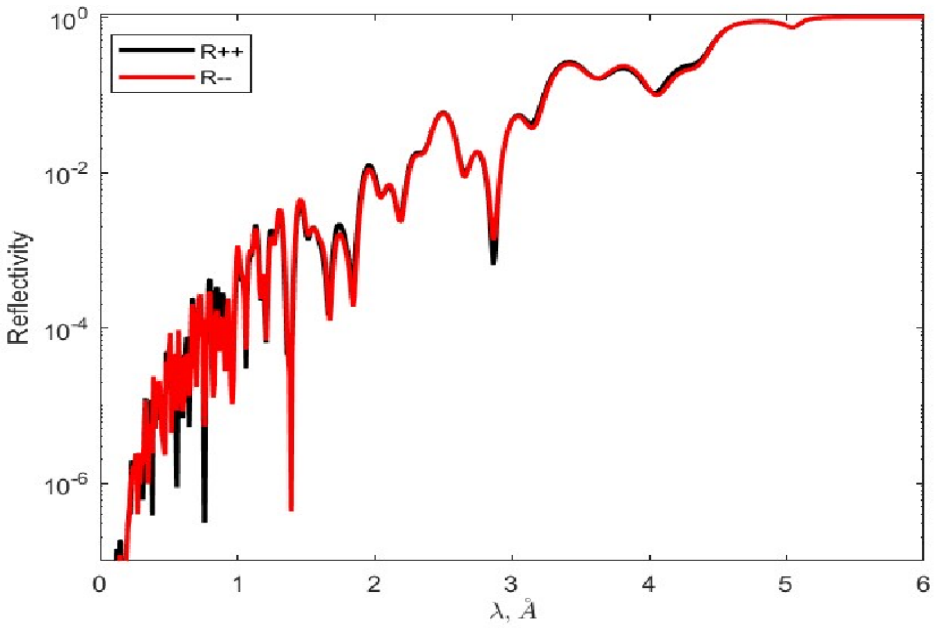

Figure 14 Neutron reflectivity for Mx, Mz (Dy)=1000 Oe

From Figure 14 we noticed that the separation between plus and minus beams is apparent for small values of magnetization and it will be more apparent for the larger magnetization magnitude.

Acknowledgement

I would like to express my thanks to my Supervisor Dr. Vladimir Zhaketov, Frank Laboratory of Neutron Physics and Joint Institute for Nuclear Research “Interest Programme” for giving me a great opportunity to excel in my learning through this project “Coexistence of Superconductivity and Ferromagnetism at Low-Dimensional Heterostructures” I have achieved a good amount of knowledge through the research & the help that I got from my Supervisor Dr. Vladimir Zhaketov, his explanation and guidance helped me in all the time of work.

References

[1] P. F. Dahl, “Kamerlingh Onnes and the Discovery of Superconductivity: The Leyden Years, 1911-1914,” *Historical Studies in the Physical Sciences*, vol. 15, no. 1, pp. 1–37, Jan. 1984,

[2] V. L. Ginzburg, “Nobel Lecture: On superconductivity and superfluidity (what I have and have not managed to do) as well as on the ‘physical minimum’ at the beginning of the XXI century,” *Rev Mod Phys*, vol. 76, no. 3, pp. 981–998, Dec. 2004,

[3] P. G. de GENNES, “Boundary Effects in Superconductors,” *Rev Mod Phys*, vol. 36, no. 1, pp. 225–237, Jan. 1964,

[4] V. L. Aksenov, Yu. v. Nikitenko, A. v. Petrenko, V. M. Uzdin, Yu. N. Khaidukov, and H. Zabel, “Features of the magnetic state of the layered Fe-V nanostructure of the superconductor-ferromagnet type,” *Crystallography Reports*, vol. 52, no. 3, pp. 381–386, May 2007,

[5] Yu. N. Khaydukov *et al.*, “Magnetic and superconducting phase diagram of Nb/Gd/Nb trilayers,” *Phys Rev B*, vol. 97, no. 14, p. 144511, Apr. 2018,

[6] Z. Radovic, M. Ledvij, L. Dobrosavljevic -Grujic, A. I. Buzdin, and J. R. Clem, “Transition temperatures of superconductor-ferromagnet superlattices,” 1991. [Online].

[7] Y. N. Proshin and M. G. Khusainov, “Manifestations of the Larkin-Ovchinnikov-Fulde-Ferrell state in bimetal ferromagnet-superconductor structures,” 1997. [Online].

[8] T. Löfwander, T. Champel, J. Durst, and M. Eschrig, “Interplay of Magnetic and Superconducting Proximity Effects in Ferromagnet-Superconductor-Ferromagnet Trilayers,” *Phys Rev Lett*, vol. 95, no. 18, p. 187003, Oct. 2005,

[9] A. Rühm, B. P. Toperverg, and H. Dosch, “Supermatrix approach to polarized neutron reflectivity from arbitrary spin structures,” *Phys Rev B*, vol. 60, no. 23, pp. 16073–16077, Dec. 1999,

[10] Y. V. Nikitenko and V. D. Zhaketov, “Magnetism in Ferromagnetic-Superconducting Layered Structures,” *Physics of Particles and Nuclei*, vol. 53, no. 6, pp. 1089–1125, Dec. 2022, [Online].

[11] M. Utsuro, V. K. Ignatovich, W. Verlag GmbH, and C. KGaA, “Neutron Optics.”

[12] V. D. Zhaketov *et al.*, “Polarized Neutron Reflectrometer with the Recording of Neutrons and Gamma Quanta,” *Journal of Surface Investigation*, vol. 15, no. 3, pp. 549–562, May 2021, [Online].

[13] S. Mironov, A. S. Mel’nikov, and A. Buzdin, “Electromagnetic proximity effect in planar superconductor-ferromagnet structures,” *Appl Phys Lett*, vol. 113, no. 2, Jul. 2018, [Online].

[14] A. V. Putilov, S. V. Mironov, A. S. Mel’nikov, and A. I. Buzdin, “Giant electromagnetic proximity effect in superconductor/ferromagnet superlattices,” Mar. 2022,

[15] L. ~b B. P. Goodman ; C, R. Bean ; ~'m, P. Schafroth ; V, ; ~ D J Grassman, I. Quinn, and % B Ittner, "laboration in the experiments and to R. Epworth and J. Hasiak for their technical assistance. We are grateful to for helpful discussions throughout the course of the present experiments. *On leave of absence from the University of Washing-ton ~Transition temperatures of the samples used in the present experiments were measured by OF FLUX CREEP IN HARD SUPERCONDUCTORS," Academic Press, Inc, 1957.

[16] N. A. Logoboy and E. B. Sonin, "Superconductivity without diamagnetism in systems with broken time-reversal symmetry," *Phys Rev B Condens Matter Mater Phys*, vol. 79, no. 2, Jan. 2009, [Online].

[17] F. S. Bergeret, K. B. Efetov, and A. I. Larkin, "Nonhomogeneous magnetic order in superconductor-ferromagnet multilayers."

[18] V. D. Zhaketov *et al.*, "Magnetic and Superconducting Properties of the Heterogeneous Layered Structures V/Fe0.7V0.3/V/Fe0.7V0.3/Nb and Nb/Ni0.65(0.81)Cu0.35(0.19)," *Journal of Experimental and Theoretical Physics*, vol. 129, no. 2, pp. 258–276, Aug. 2019,

[19] D. I. Devyaterikov *et al.*, "Influence of Dimensional Effects on the Curie Temperature of Dy and Ho Thin Films," *Physics of Metals and Metallography*, vol. 122, no. 5, pp. 465–471, May 2021,

[20] Yu. N. Khaydukov *et al.*, "Magnetic proximity effect in Nb/Gd superlattices seen by neutron reflectometry," *Phys Rev B*, vol. 99, no. 14, p. 140503, Apr. 2019, [Online].